Fibroblast Growth Factor 21 Improves Insulin Resistance and Ameliorates Renal Injury in *db/db* Mice

H. W. Kim, J. E. Lee, J. J. Cha, Y. Y. Hyun, J. E. Kim, M. H. Lee, H. K. Song, D. H. Nam, J. Y. Han, S. Y. Han, K. H. Han, Y. S. Kang, and D. R. Cha

Department of Internal Medicine (H.W.K., J.E.L.), Wonkwang University, Gunpo 570–479, South Korea; Department of Internal Medicine (J.J.C., J.E.K., M.H.L., H.K.S., D.H.N., Y.S.K., D.R.C.), Korea University Ansan Hospital, Ansan 425–020, South Korea; Department of Internal Medicine (Y.Y.H.), Sungkyunkwan University Kangbuk Samsung Hospital, Seoul 135–710, South Korea; Department of Pathology (J.Y.H.), Inha University Hospital, Incheon 402–751, South Korea; and Department of Internal Medicine (S.Y.H., K.H.H.), Division of Nephrology, Inje University, Goyang 411-706, South Korea

Despite the emerging importance of fibroblast growth factor 21 (FGF21) as a metabolic hormone regulating energy balance, its direct effects on renal function remain unexplored. FGF21 was injected ip daily for 12 weeks into *db/db* mice. Compared with control vehicle injection, FGF21 treatment significantly improved lipid profiles and insulin resistance and resulted in significantly higher serum adiponectin levels. In contrast, serum insulin and 8-isoprostane levels were significantly decreased. Interestingly, FGF21 and its receptor components in the kidneys were found to be significantly up-regulated in *db/db* mice, which suggests an FGF21-resistant state. FGF21 treatment significantly down-regulated FGF21 receptor components and activated ERK phosphorylation. FGF21 administration also markedly decreased urinary albumin excretion and mesangial expansion and suppressed profibrotic molecule synthesis. Furthermore, FGF21 improved renal lipid metabolism and oxidative stress injury. In cultured renal cells, FGF21 was mainly expressed in mesangial cells, and knockdown of FGF21 expression by stealth small interfering RNA further aggravated high-glucose-induced profibrotic cytokine synthesis in mesangial cells. Our results suggest that FGF21 improves insulin resistance and protects against renal injury through both improvement of systemic metabolic alterations and antifibrotic effects in type 2 diabetic nephropathy. Targeting FGF21 could therefore provide a potential candidate approach for a therapeutic strategy in type 2 diabetic nephropathy. **(*Endocrinology* 154: 3366–3376, 2013)**

Fibroblast growth factor 21 (FGF21) is a member of the fibroblast growth factor family and has been identified as an important regulator of energy metabolism (1). The role of FGF21 in metabolic regulation was first demonstrated as facilitating glucose uptake by adipocytes through up-regulating transcription of the glucose transporter-1 (2). The same study reported that overexpression of FGF21 in the liver of transgenic mice improved insulin sensitivity, glucose clearance, and resistance to weight gain despite a significant increase in caloric intake, whereas others indicated that adenoviral knockdown of FGF21 in mice leads to fatty liver and a marked increase in triglyceride levels (2, 3). Taken together, in terms of both efficacy and safety, FGF21 could be an excellent candidate for a therapeutic strategy in obesity-related diabetic conditions.

Previous studies have demonstrated that various types of fibroblast growth factor receptors (FGFRs) are also expressed and localized in adult as well as developing murine kidneys (4, 5). Taken together, these findings suggest

ISSN Print 0013-7227 ISSN Online 1945-7170
Printed in U.S.A.

Received December 27, 2012. Accepted June 27, 2013.
First Published Online July 3, 2013

Abbreviations: DIO, diet-induced obesity; FGF21, fibroblast growth factor 21; FGFR, fibroblast growth factor receptor; HbA1c, glycosylated hemoglobin; HOMA-IR, homeostasis model insulin resistance assessment index; LDL, low-density lipoprotein; LPO, lipid hydroperoxide; MC, mesangial cell; NF-κB, nuclear factor-κB; PAI-1, plasminogen activator inhibitor-1; PI3K, phosphatidylinositide 3-kinase; RNAi, RNA interference; siRNA, small interfering RNA.

that the kidneys may not only be one of the target organs for FGF21 expression but also may be protected against obesity-related diabetic injury by the treatment of FGF21. To date, there has been no convincing demonstration of this association. In this study, we administered recombinant FGF21 to *db/db* mice and observed its effects on changes in diabetes-related parameters and specifically in renal functional and morphologic changes. We also carried out in vitro experiments to investigate the molecular mechanism of direct renal effects of FGF21.

Materials and Methods

Animal experiments

Six-week-old male diabetic *db/db* mice (C57BLKS/J-*lepr*^{db}/*lepr*^{db}) and male nondiabetic *db/m* mice (C57BLKS/J-*lepr*^{db}/+) were purchased from Jackson Laboratory (Sacramento, California). Recombinant FGF21 was purchased from Phoenix Pharmaceutical, Inc (Belmont, California). The mice were treated with FGF21 at the age of 8 weeks, and all mice were kept at controlled temperature (23°C ± 2°C) and humidity (55% ± 5%) levels under an artificial light cycle. The mice were divided into 3 groups. The first group consisted of nondiabetic *db/m* mice as nondiabetic controls (n = 4), the second group was composed of vehicle-treated diabetic *db/db* mice (n = 8), and the third group was made up of diabetic *db/db* mice treated with FGF21 by daily ip injection for 3 months at a dose of 25 μg/kg·d (n = 8). We selected this dose of FGF21 because previous studies showed that a minimum dose within 10–100 μg/kg·d was required for in vivo FGF21 activity in diet-induced obese mice and *ob/ob* mice (2, 6).

Food intake, water intake, urine volume, body weight, glycosylated hemoglobin (HbA1c), and fasting plasma glucose concentration were measured monthly during the experiment. Plasma glucose levels were measured using a glucose oxidase-based method, HbA1c levels were calculated by the IN2IT system (Bio-Rad Laboratories, Hercules, California), and creatinine levels were determined by HPLC. Plasma insulin levels and plasma adiponectin levels were measured with an ELISA kit (Linco Research, St Charles, Missouri). Plasma FGF21 concentration was measured with an ELISA kit (R&D Systems Inc, Minneapolis, Minnesota). The homeostasis model insulin resistance assessment index (HOMA-IR) was calculated using the formula of fasting glucose (millimoles per liter) × fasting insulin (milliunits per unit)/22.5. Plasma triglyceride and cholesterol analyses were performed using a GPO-Trinder kit (Sigma-Aldrich, St Louis, Missouri). Plasma lipoprotein profiles were measured using a fast protein liquid chromatography (HPLC) system. Insulin tolerance testing (ITT) was conducted in *db/db* mice after 8 hours of fasting, and blood samples were collected through the tail vein. Mice received 0.75 U/kg regular insulin by ip injection, and blood glucose was subsequently measured at 0, 30, 60, 90, and 120 minutes. Plasma and urinary levels of 8-isoprostane were measured with an ELISA kit (Cayman Chemical, Ann Arbor, Michigan). Lipids from the hepatic, adipose, and renal cortical tissues were extracted as described by Bligh and Dyer (7). Total cholesterol and triglyceride contents were measured using a commercial kit (Wako Chemicals, Richmond, Virginia). The extent of peroxidative reaction in the hepatic, adipose tissue, and kidneys was determined by directly measuring lipid hydroperoxides (LPOs) using an LPO assay kit (Cayman Chemical) as described previously (8).

To determine urinary albumin excretion, individual mice were caged once per month in a metabolic cage and urine was collected for 24 hours. Urinary albumin concentrations were determined by competitive ELISA (Shibayagi, Shibukawa, Japan). After 3 months of treatment, mice were euthanized under anesthesia by ip injection of sodium pentobarbital (50 mg/kg). Epididymal fat, liver, and kidney tissues were weighed and subsequently snap frozen in liquid nitrogen. All experiments were conducted in accordance with National Institutes of Health guidelines and with approval of the Korea University Institutional Animal Care and Use Committee.

Analysis of gene expression by real-time quantitative PCR

Total RNA was extracted from the renal cortical tissues, adipose tissue, and experimental cells with TRIzol reagent and further purified using an RNeasy minikit (QIAGEN, Valencia, California). Primer sequences are listed in Supplemental Table 1, published on The Endocrine Society's Journals Online web site at http://endo.endojournals.org. Quantitative gene expression was performed on a LightCycler 1.5 system (Roche Diagnostics Corp, Indianapolis, Indiana) using SYBR Green technology. In brief, 10 μL of SYBR Green master mix was added to 1 μL of RNA (corresponding to 50 ng of total RNA) and 900 nmol/L of forward and reverse primers in a reaction volume of 20 μL. Real-time RT-PCR was performed for 10 minutes at 50°C, 5 minutes at 95°C, and a total of 22–30 cycles of 10 seconds at 95°C and 30 seconds at 60°C. Samples were finally heated to 95°C to verify that a single PCR product had been obtained. The ratio of the expression level of each gene to that of the β-actin level (relative gene expression number) was calculated by subtracting the threshold cycle number of the target gene from that of β-actin and raising 2 to the power of this difference.

Histopathological evaluation and immunohistochemistry

Kidney and adipose tissues were fixed for 48 hours with 10% paraformaldehyde at 4°C, dehydrated, embedded in paraffin, cut into 4-μm-thick slices, and stained with periodic acid-Schiff and hematoxylin and eosin. Glomerular mesangial expansion was scored semiquantitatively, and the percentage of mesangial matrix occupying each glomerulus was rated 0–4 as follows: 0, 0%; 1, less than 25%; 2, 25%–50%; 3, 50%–75%; and 4, more than 75%. For immunohistochemical staining, renal tissues were sliced into 4-μm sections. Slides were transferred to a 10-mmol/L citrate buffer solution at pH 6.0 and heated at 80°C for 30 minutes for TGF-β_1, fibronectin, and laminin. For type IV collagen staining, slides were treated with trypsin (one tablet per 1 mL of water) for 20 minutes for antigen retrieval. To block endogenous peroxidase activity, 3.0% H_2O_2 in methanol was applied for 20 minutes, followed by incubation at room temperature for 60 minutes in 3% BSA/3% normal goat serum (type IV collagen, fibronectin, and laminin) or 30 minutes in 20% normal sheep serum (TGF-β_1). Slides were incubated overnight at 4°C with a rabbit polyclonal anti-TGF-β1 antibody (1:100; Santa Cruz Biotechnology, Santa Cruz, California), rabbit polyclonal antitype

IV collagen antibody (1:150; BioDesign International, Sarco, Maine), rabbit polyclonal antifibronectin antibody (1:100; Abcam Plc, Cambridge, Massachusetts), or rat monoclonal antilaminin antibody (1:50; Abcam). Slides were incubated in secondary antibodies for 30 minutes, and at room temperature in 0.05% 3,30-diaminobenzidine containing 0.01% H_2O_2 before counterstaining with Mayer's hematoxylin. For the evaluation of immunohistochemical staining for type IV collagen, TGFβ1, fibronectin, and laminin, glomerular fields were graded semiquantitatively using a high-power field containing 50–60 glomeruli, and an average score was calculated as described previously (9). A pathologist carried out the histological examinations in a blinded manner.

Protein extraction and Western blot analysis

Nuclear and cytoplasmic proteins were extracted from renal cortical tissues and cells using a commercial nuclear extraction kit according to the manufacturer's instructions (Active Motif, Carlsbad, California). Protein concentrations were determined using the bicinchoninic acid method (Pierce Pharmaceuticals, Rockford, Illinois). For Western blotting, 40 μg of protein was electrophoresed on a 10% SDS-PAGE minigel. Proteins were transferred onto a polyvinylidene difluoride membrane, and the membrane was hybridized in blocking buffer overnight at 4°C with rabbit polyclonal anti-FGF21 antibody (1:1000; Abcam), mouse monoclonal anti-nuclear factor-κB (NF-κB) p65 antibody (1:1000; Cell Signaling Technology, Beverly, Massachusetts), rabbit polyclonal antiplasminogen activator inhibitor-1 (PAI-1) antibody (1:500; Santa Cruz Biotechnology), sterol-regulatory element-binding protein-1c antibody (1:500, Santa Cruz Biotechnology), rabbit polyclonal anti-ATP-binding cassette transporter 1 antibody (1:200, Santa Cruz Biotechnology), rabbit polyclonal anti-TGFβ1 antibody (1:200; Santa Cruz Biotechnology), phospho-specific ERK1/2, total ERK1/2 (1:1000, New England Biolabs, Inc, Beverly, Massachusetts), type IV collagen antibody (1:500, Santa Cruz Biotechnology), or mouse monoclonal anti-TATA binding protein antibody (1:1000; Abcam). The membrane was subsequently incubated with horseradish peroxidase-conjugated secondary antibody (1:1000 dilution) for 60 minutes at room temperature. Specific signals were detected using the enhanced chemiluminescence method (Amersham, Buckinghamshire, United Kingdom)

Mesangial cell culture and stealth RNA interference (RNAi) for FGF21

Because FGF21 was preferentially detected in mesangial cells (MCs), we used MCs to elucidate the molecular mechanism of FGF21. A portion of the renal cortex from normal C57BL/6 mice was obtained immediately after surgical nephrectomy and glomeruli were isolated using the differential sieving method. MCs were cultured in DMEM supplemented with 10% fetal calf serum. With the use of indirect immunofluorescence staining, the MCs were identified due to their large stellate shape and the positive staining for α-smooth muscle actin but negative staining for synaptopodin, common leukocyte antigen, and E-cadherin. To evaluate the effect of high glucose on FGF21 synthesis, subconfluent MCs were serum starved for 24 hours, and the medium was then exchanged with media containing 30 mM D-glucose for 48 hours. Because FGF21 showed a beneficial effect in renal function, we next used small interfering RNA (siRNA) directed against FGF21 to investigate whether FGF21 regulated fibrotic molecule synthesis. Mouse FGF21 mRNA was specifically knocked down using commercially available siRNA oligonucleotides. The sequences of the stealth siRNAs were designed using BLOCK-iT RNAI Designer (Invitrogen Life Technologies, Gaithersburg, Maryland): sense strand, 5′-CAA GUC CGG CAG AGG UAC CUC UAC A-3′; antisense strand, 5′-UGU AGA GGU ACC UCU GCC GGA CUU G-3′. The MCs were maintained in DMEM with 10% fetal calf serum before transfection with 10 nmol siRNA using Lipofectamine RNAiMax (Invitrogen Life Technologies) according to the manufacturer's instructions. MCs were transfected for 24 hours with siRNA and cultivated in serum-free and antibiotic-free DMEM. Cells were made quiescent for 24 hours and treated with 30 mM high-glucose medium for 72 hours. The stealth RNAi-negative control duplexes were used as controls.

Statistical analysis

A nonparametric analysis was used because of the relatively few samples. Results were expressed as the mean ± SEM. Multiple comparisons were done using Wilcoxon rank sum tests and Bonferroni correction. A Kruskal-Wallis test compared more than 2 groups, followed by a Mann-Whitney *U* test, using a microcomputer-assisted program with SPSS for Windows 10.0 (SPSS, Chicago, Illinois). A value of $P < .05$ was considered statistically significant.

Results

Biochemical and physical measurements in experimental animals

Table 1 shows the various biochemical and physical parameters measured in experimental animals. Levels of fasting blood glucose, HbA1c, body weight, urine volume, water and food intake, and fat and liver mass per body weight were significantly higher in diabetic *db/db* than in nondiabetic *db/m* mice. On the other hand, when compared with vehicle-treated *db/db* mice, FGF21-treated *db/db* mice showed significantly reduced mass of kidney, liver, and epididymal fat per body weight but no significant differences in the levels of fasting blood glucose, HbA1c, urine volume, water and food intake, and plasma concentrations of creatinine. Plasma FGF21 concentrations were elevated 20-fold in diabetic *db/db* mice compared with those in control *db/m* mice. Interestingly, FGF21 treatment significantly decreased plasma FGF21 levels (Table 1).

Metabolic parameters in experimental animals

As shown in Figure 1, *db/db* mice had significantly higher levels of plasma insulin and HOMA-IR compared with control *db/m* mice. Interestingly, FGF21 treatment induced a significant improvement in these parameters. Insulin tolerance testing confirmed that FGF21 improved the insulin resistance state (Figure 1A). In accordance with

Table 1. Physical and Biochemical Parameters of Experimental Animals

Parameters	Week	*db/m* Control	*db/db*+Vehicle	*db/db*+FGF21
Body weight, g	0	26.25 ± 0.63	37.37 ± 0.82[a]	38.25 ± 0.83[a]
	4	28.25 ± 0.85	48.50 ± 1.64[b]	51.62 ± 2.52[b]
	8	32.00 ± 1.08	56.00 ± 1.59[b]	51.25 ± 3.25[b]
	12	33.25 ± 1.31	61.00 ± 2.05[b]	52.00 ± 3.83[b]
Daily food intake, g	0	2.37 ± 0.36	5.18 ± 0.67[b]	5.31 ± 0.28[b]
	4	2.56 ± 0.18	5.21 ± 0.34[b]	4.75 ± 0.34[b]
	8	3.12 ± 0.36	5.00 ± 0.15[a]	5.62 ± 0.15[b]
	12	2.87 ± 0.21	5.31 ± 0.13[b]	5.68 ± 0.20[b]
Daily water intake, g	0	5.50 ± 0.43	14.06 ± 1.42[b]	12.68 ± 1.43[b]
	4	6.25 ± 0.43	14.68 ± 0.77[b]	11.62 ± 0.82[a]
	8	6.37 ± 1.37	14.75 ± 1.23[b]	15.06 ± 0.28[b]
	12	6.25 ± 0.72	18.68 ± 0.75[b]	17.50 ± 0.51[b]
Fasting blood glucose, mmol/L	0	9.4 ± 0.4	29.0 ± 0.9[b]	31.1 ± 0.9[b]
	4	8.9 ± 0.6	30.9 ± 1.9[b]	30.3 ± 1.5[b]
	8	10.7 ± 0.4	32.1 ± 1.8[b]	35.4 ± 2.9[b]
	12	7.8 ± 0.1	36.7 ± 1.5[b]	36.0 ± 1.9[b]
HbA1c, %	0	5.40 ± 0.16	8.61 ± 0.25[b]	9.58 ± 0.41[b]
	4	5.02 ± 0.25	9.92 ± 0.38[b]	10.72 ± 0.64[b]
	8	4.87 ± 0.10	10.31 ± 0.33[b]	13.03 ± 1.44[b]
	12	5.05 ± 0.25	12.40 ± 0.31[b]	12.15 ± 0.45[b]
UV, mL/d	0	1.62 ± 0.44	3.97 ± 0.34[c]	4.44 ± 0.34[a]
	4	1.16 ± 0.27	3.55 ± 0.39[a]	4.30 ± 0.80[a]
	8	0.66 ± 0.14	5.13 ± 0.44[b]	3.42 ± 0.64[a]
	12	0.44 ± 0.21	4.00 ± 0.52[b]	3.52 ± 0.72[a]
Kidney per 100 g BW	12	1.71 ± 0.06	1.38 ± 0.07	1.03 ± 0.15[a,d]
Heart per 100 g BW	12	0.76 ± 0.02	0.46 ± 0.01[a]	0.45 ± 0.10[a]
Fat per 100 g BW	12	3.43 ± 0.89	8.19 ± 0.41[b]	5.07 ± 0.36[c,e]
Liver per 100 g BW	12	5.87 ± 0.24	9.11 ± 0.63[a]	5.44 ± 0.23[e]
Adiponectin, μg/mL	12	2.76 ± 0.13	2.52 ± 0.16[c]	2.68 ± 0.05[d]
P-8-isoprostane, pg/mL	12	475 ± 122	1309 ± 183[c]	598 ± 186[d]
P-creatinine, μmol/L	12	7.0 ± 3.0	8.0 ± 1.0	7.0 ± 3.0
P-FGF21, pg/mL	12	78.3 ± 12.3	1513 ± 218[b]	935 ± 156[b,d]

Abbreviations: BW, body weight; P, plasma; UV, urine volume. Values are expressed as means ± SEM. Statistical analysis was performed between groups at the same time periods.

[a] $P < .01$ vs *db/m* control.

[b] $P < .001$ vs *db/m* control.

[c] $P < .05$ vs *db/m* control.

[d] $P < .05$ vs *db/db* + vehicle.

[e] $P < .001$ vs *db/db* + vehicle.

these changes, plasma levels of total cholesterol, triglycerides, and low-density lipoprotein (LDL) cholesterol were significantly higher in diabetic *db/db* than in nondiabetic *db/m* mice, but these increases were significantly ameliorated by FGF21 treatment when compared with vehicle-treated *db/db* mice. In addition, the serum level of adiponectin, an adipokine possessing antiinflammatory and antidiabetic properties, was significantly increased by FGF21 treatment (Table 1).

Effects of FGF21 treatment on changes in histological and adipocytokine mRNA expression in epididymal adipose tissue in experimental animals

Adipose tissue dysfunction is now considered to play a central role in obesity and its associated disorders and is characterized in part by changes in adipocyte volume and mRNA expression patterns of various adipokines (10). We therefore investigated whether these changes were influenced by FGF21 treatment. Epididymal adipose tissue of *db/db* mice had larger adipocytes than *db/m* mice, and FGF21 treatment restored their hypertrophic phenotype to the small differentiated phenotype, which was consistent with the finding of reduced epididymal fat mass per body weight after FGF21 treatment (Supplemental Figure 1A and Table 1). In accordance with this morphological alteration, mRNA expression levels of proinflammatory and profibrotic adipokines were remarkably up-regulated in the fat pad of *db/db* mice compared with *db/m* mice, whereas mRNA expression levels of antiinflammatory or adipocyte differentiation-related molecules were down-regulated (Supplemental Figure 1B). Among these changes in adipose tissue mRNA levels, expression of both PAI-1

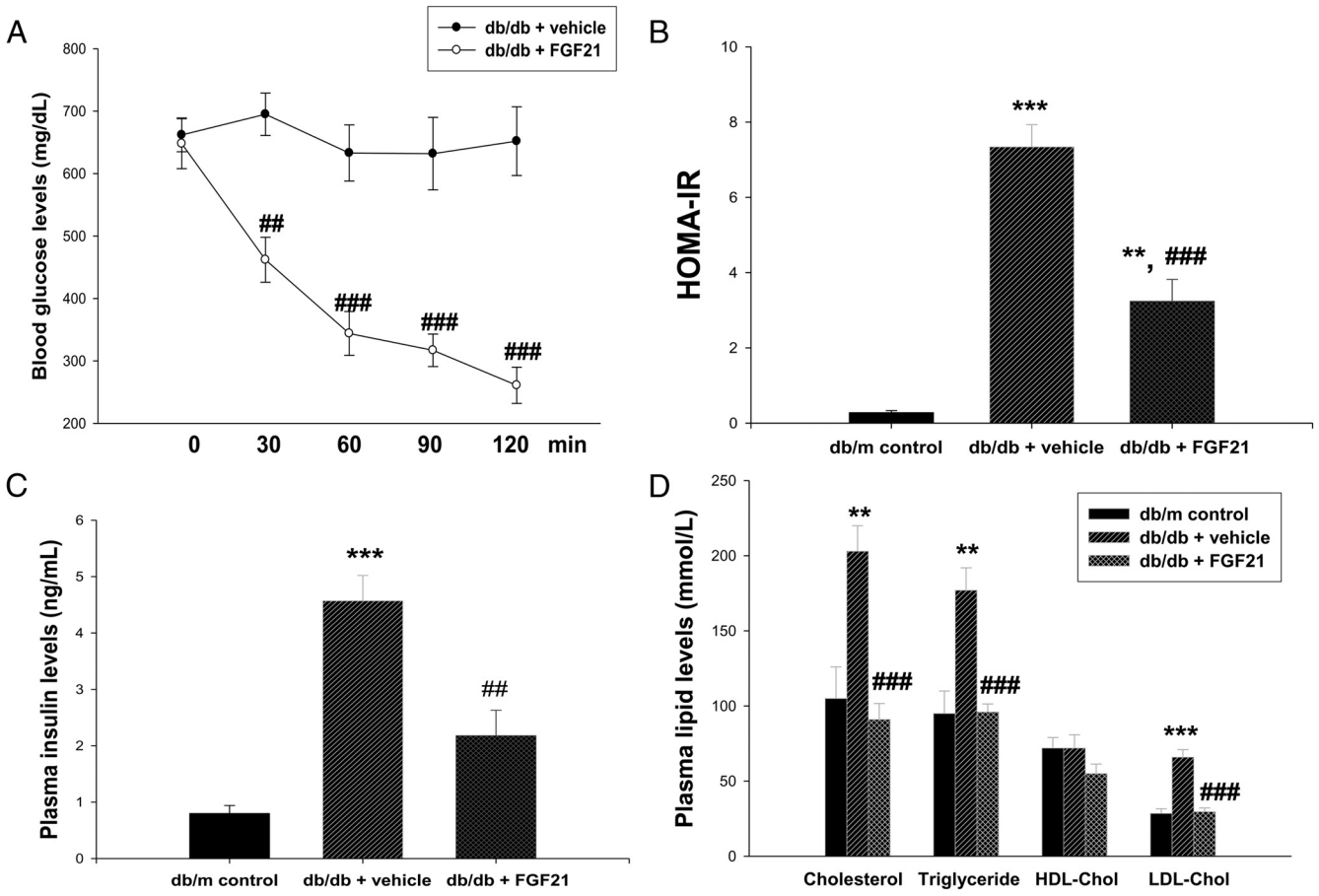

Figure 1. Effect of FGF21 on insulin resistance and lipid parameters at 20 weeks in experimental animals. Insulin tolerance tests (A), HOMA-IR (B), plasma insulin concentration (c), and plasma lipid concentration (D) are shown. HDL-Chol, HDL-cholesterol; LDL-Chol, LDL-cholesterol. Data are expressed as the mean ± SEM. **, $P < .01$, ***, $P < .001$ vs *db/m* control; ##, $P < .01$, ###, $P < .001$ vs *db/db* + vehicle.

and TNF-α were significantly reduced in FGF21- compared with vehicle-treated mice. In contrast, mRNA levels of adiponectin and peroxisomal proliferator-activated receptor-γ were significantly enhanced by FGF21 treatment (Supplemental Figure 1B).

Effects of FGF21 treatment on renal functional and structural changes in experimental animals

Throughout the experimental period, urinary albumin excretion was significantly increased in *db/db* mice as compared with *db/m* mice. This increase in albuminuria was significantly attenuated by 8 weeks of FGF21 treatment, and the decrease was maintained until 12 weeks of treatment (Figure 2). In addition, histological sections of kidneys from vehicle-treated *db/db* mice showed signs of glomerular tuft hypertrophy and mesangial expansion compared with *db/m* mice, and these changes were significantly attenuated by FGF21 treatment (Supplemental Figure 2 and Figure 3). Consistent with these histological changes, mRNA expression levels of type IV collagen, PAI-1, and TGF-β_1 were increased in vehicle-treated *db/db* compared with *db/m* mice, and this increase in expression of profibrotic cytokine genes was significantly reduced by FGF21 treatment (Figure 3). Immunohistochemical stains for profibrotic markers such as type IV collagen, TGF-β_1, laminin, and fibroncetin showed similar tendencies. Semiquantitative immunostaining scores for all these markers were significantly increased in vehicle-treated *db/db* compared with *db/m* mice, and all of these profibrotic changes were also significantly ameliorated by FGF21 treatment. These results demonstrated that FGF21 treatment significantly ameliorated functional (urinary albumin excretion) and morphological glomerular abnormalities induced by chronic diabetic injury in *db/db* mice.

Lipid peroxidation and oxidative stress parameters in experimental animals

Oxidative stress, referred to as an imbalance between reactive oxygen species and antioxidants, has been regarded as a major contributor to obesity-related diabetic morbidities (11). Lipid peroxidation and its bioactive product, isoprostanes, are the most extensively studied markers of diabetes-related free radical attacks (12, 13). Because FGF21 treatment improved insulin resistance and dyslipidemia, and possibly reduced oxidative stress, we

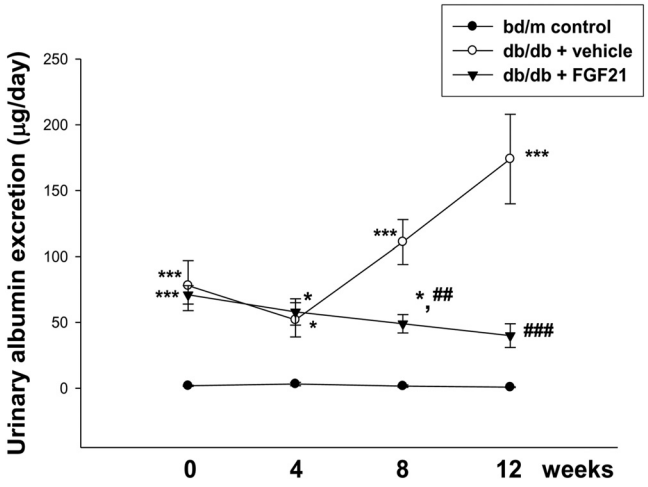

Figure 2. Effects of FGF21 on 24-hour urinary albumin excretion in experimental animals. A 24-hour urine sample was collected at monthly intervals after FGF21 administration. Statistical analysis was performed between groups at the same time periods. Data are means ± SEM. *, $P < .05$, ***, $P < .001$ vs *db/m* control; ##, $P < .01$, ###, $P < .001$ vs *db/db* + vehicle.

next evaluated whether FGF21 treatment also affected these parameters including lipotoxicity in the kidney by measuring the changes in serum and urinary levels of 8-isoprostane, the tissue level of LPO and tissue lipid accumulation. As expected, plasma levels of 8-isoprostane were 3 times higher in *db/db* mice than in *db/m* mice, and these increases were abrogated by FGF21 treatment (Table 1). FGF 21 treatment also decreased cholesterol and triglyceride accumulation in the diabetic kidney (Figure 4), which has been proposed to play an important role in the progression of diabetic nephropathy (14, 15). In addition, urinary 8-isoprostane levels and kidney LPO levels were markedly increased in *db/db* compared with *db/m* mice, and these increases were significantly attenuated by FGF21 treatment (Figure 4). Finally, to explore the mechanism of the beneficial effects of FGF21 treatment on diabetic renal injury, we determined the change in nuclear p65 protein expression, which reflects activity of NF-κB, a key mediator of obesity-related inflammation. Western blot analysis in extracted renal cortical nuclear proteins demonstrated that there was an increase in p65 protein level in renal tissues of *db/db* mice compared with lean *db/m* mice, and FGF21 treatment markedly abolished this increase (Figure 5A). This finding suggests that the antidiabetic properties of FGF21 are, at least in part, mediated by suppression of the proinflammatory NF-κB pathway. Because FGF21 treatment improved renal lipid contents and oxidative stress, we next examined whether improvement in renal function originated from the correction of alteration in renal lipid metabolism. Specifically we measured mRNA expression levels of genes known to be involved in lipid synthesis and cholesterol efflux. As shown in Figure 5B, FGF21 treatment dramatically suppressed gene expression of both sterol-regulatory element-binding protein-1c and 3-hydroxy-3-methylglutaryl-coenzyme A reductase, which induces lipid synthesis. Furthermore, gene expression of ATP-binding cassette transporter A1, which modulates cholesterol efflux, was significantly increased by FGF21 treatment. These findings were in agreement with the results that FGF21 decreased renal cholesterol and triglyceride levels (Figures 4–6).

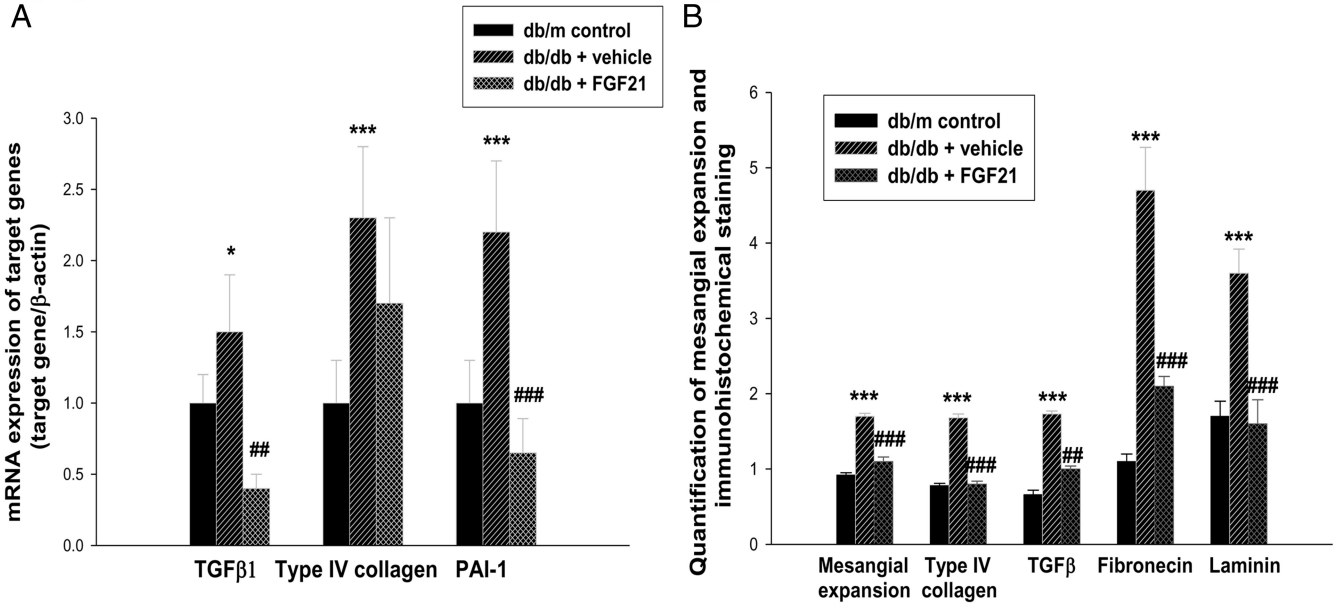

Figure 3. Effect of FGF21 on profibrotic molecule synthesis in renal cortical tissues. A, mRNA expression of renal cortical tissues. B, Glomerular mesangial expansion score and immunostaining score. Data are shown as the mean ± SEM. *, $P < .05$, ***, $P < .001$ vs *db/m* control; ##, $P < .01$, ###, $P < .001$ vs *db/db* + vehicle.

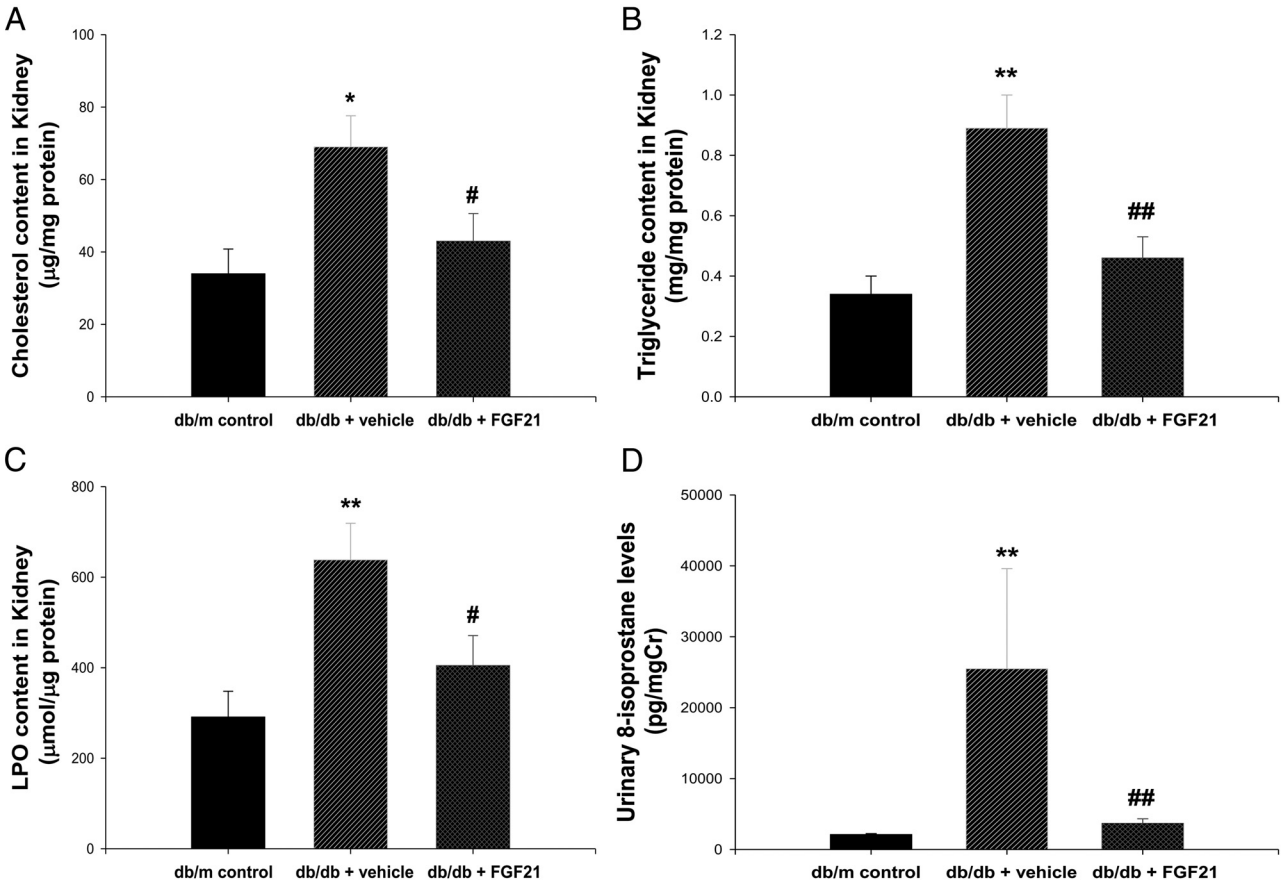

Figure 4. Effects of FGF21 on renal lipid metabolism, lipid peroxidation, and oxidative stress in experimental animals. A, Cholesterol content in renal cortical tissue. B, Triglyceride content in renal cortical tissue. C, LPO content in renal cortical tissue. D, Twenty-four-hour urinary levels of 8-isoprostane; urinary excretion of 8-isoprostane was corrected by urinary creatinine. Data are means ± SEM. *, $P < .05$, **, $P < .01$ vs *db/m* control; #, $P < .05$, ##, $P < .01$ vs *db/db* + vehicle.

Expression of FGF21 in diabetic kidneys and cultured mesangial cells

Because FGF21 has been reported to be expressed in various tissues, we examined whether FGF21 was synthesized by various renal cells. FGF21 expression was investigated in renal cells in the untreated basal state by real-time quantitative PCR and Western blot. We tested cultured immortalized podocytes, primary cultured mouse MCs, and immortalized human renal proximal tubule cells (HK2 cells) and found that FGF21 was expressed exclusively in mesangial cells and not in podocytes and HK2 cells (Supplemental Figure 3). Next, we examined the effect of high glucose (30 mM) stimulation on FGF21 synthesis in MCs. As shown in Supplemental Figure 4, high glucose stimulation did not induce significant change in FGF21 expression. In addition, we performed Western blot analysis from renal lysates to elucidate whether there is altered renal FGF21 signaling in diabetic kidney compared with that in control kidney. As shown in Supplemental Figure 5, we observed that ERK phosphorylation was decreased in diabetic *db/db* mice compared with *db/m* mice. We further evaluated whether FGF21-related components including β-Klotho and FGF21 receptor were changed in the diabetic kidney. As shown in Figure 7, FGF21-related components were significantly up-regulated in diabetic *db/db* compared with *db/m* mice. Interestingly, the difference in renal expression of FGF21 was more dramatic at 20 weeks of age (Figure 7B), which suggested that the diabetic kidney was in an FGF21-resistant state. Furthermore, FGF21 treatment significantly suppressed FGF21 components such as β-Klotho, FGFR1c, and FGFR2c (Figure 7). Because FGF21 binds to FGF receptors in the presence of coreceptor β-Klotho before leading to activation of extracellular MAPK-1 and -2 (ERK1/2), we investigated whether ERK activation occurred in the FGF21-treated diabetic kidney. We found that FGF21 treatment significantly activated ERK phosphorylation in the kidney (Figure 6).

Effects of FGF21 inhibition by FGF21 knockdown on profibrotic molecule synthesis in cultured mesangial cells

Because FGF21 was preferentially activated in MCs, we performed an in vitro silencing experiment using mouse MCs. As shown in Supplemental Figure 6, silencing of FGF21 induced a reduction in FGF21 expression and further aggravated high-glucose-induced up-regulation of the synthesis of profibrotic molecules.

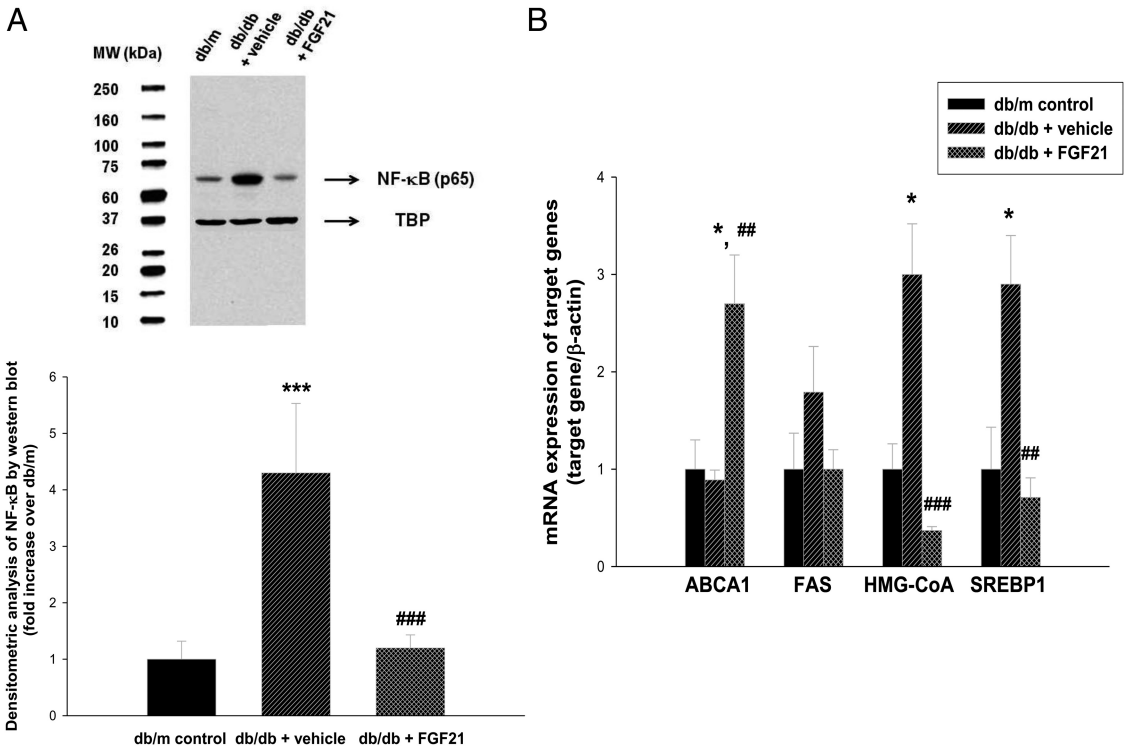

Figure 5. Effects of FGF21 on NK-κB activation and mRNA expression of genes involved in lipid metabolism in renal cortical tissues. A, Representative Western blot of NF-κB (p65) and densitometric analysis of Western blot results in renal cortical tissues. B, mRNA expression of genes related to lipid metabolism. ABCA1, ATP-binding cassette transporter-1; FAS, fatty acid synthase; HMG-CoA, cholesterol 3-hydroxy-3-methylglutaryl-CoA reductase; SREBP-1, sterol regulatory element-binding protein-1; TBP, TATA binding protein. Data are means ± SEM. *, $P < .05$, ***, $P < .001$ vs *db/m* control; ##, $P < .01$, ###, $P < .001$ vs *db/db* + vehicle.

Discussion

Because type 2 diabetes mellitus accounts for 90% of all diabetes and is closely related to obesity-related insulin resistance, numerous studies have elaborated on a potential link between obesity and diabetic kidney injury (16, 17). Among the various proposed mechanisms to explain obesity-inducing kidney injury, accumulating evidences support the roles of obesity-related circulating bioactive

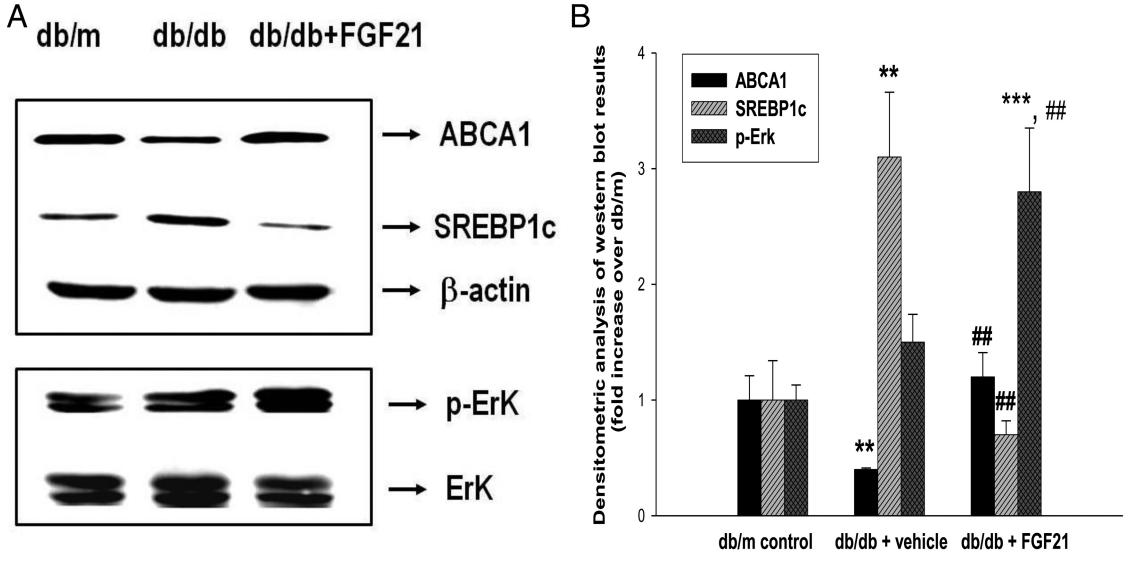

Figure 6. Representative Western blot and densitometric analysis of Western blot results in renal cortical tissues. A, Representative Western blot for ABCA1, SREBP-1c, and ERK1/2 phosphorylation. B, Densitometric analysis of Western blot results. ABCA1, ATP-binding cassette transporter-1; FAS, fatty acid synthase; SREBP-1, sterol regulatory element-binding protein-1; ERK 1/2, extracellular MAPK 1 and 2 (ERK1/2). Data are means ± SEM. **, $P < .01$, ***, $P < .001$ vs *db/m* control; ##, $P < .01$ vs *db/db* + vehicle.

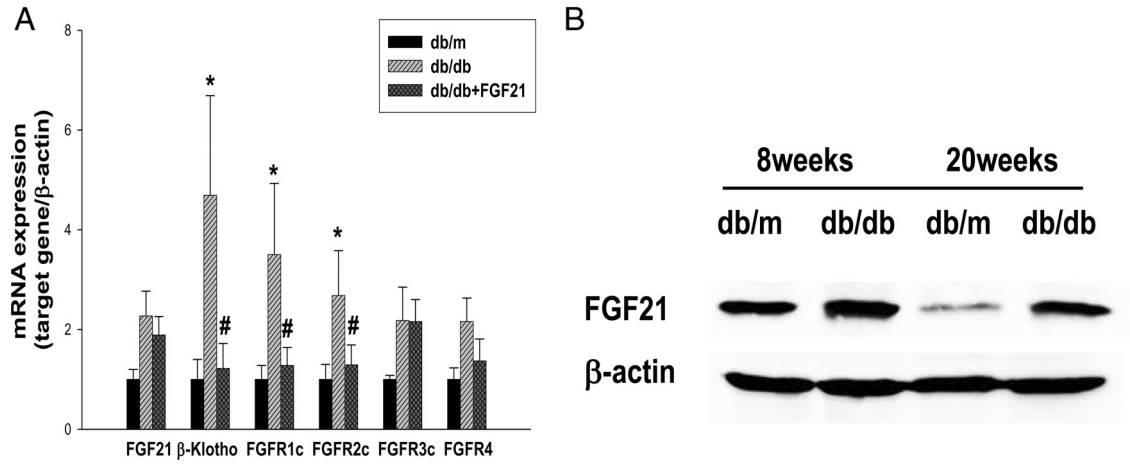

Figure 7. mRNA expression of FGF21 components and representative Western blot for FGF21 in renal cortical tissues. A, mRNA expression of FGF21, β-Klotho, FGFR1c, FGFR2c, FGFR3c, and FGFR4. B, Representative Western blot for FGF21 at 8 and 20 weeks of age in renal cortical tissues in nondiabetic *db/m* and diabetic *db/db* mice. Data are means ± SEM. *, $P < .05$ vs *db/m* control; #, $P < .05$ vs *db/db* + vehicle.

substances (18). However, the renal protective effects of FGF21 in type 2 diabetic nephropathy have not been fully investigated.

We observed that FGF21 treatment also improved insulin resistance. These results were in agreement with previous reports showing that FGF21 improves obesity-related metabolic alterations in human and experimental animals (19, 20). In this study, we found that FGF21 treatment significantly ameliorated obesity-induced increases in proinflammatory adipocytokines such as PAI-1 and TNF-α in adipose tissue as well as enhancing antiinflammatory and antidiabetic molecules such as adiponectin and peroxisomal proliferator-activated receptor-γ.

In this study we observed that exogenous administration of FGF21 improved dyslipidemia as well as metabolic abnormalities. In addition, FGF21 treatment significantly reduced the obesity-induced increase in fat and liver weight per body weight. This is in agreement with a previous study that showed that FGF21 treatment modulates triglyceride secretion and improvement of hepatosteatosis (19). More recent research has also demonstrated that FGF21 can augment the action of statin in liver, which ultimately leads to lower blood LDL-cholesterol (21). On the other hand, the body weight of FGF21-treated mice did not decrease in comparison with vehicle-treated mice. As previously reported, the weight-lowering effect of FGF21 is dependent on the administered dose, which in the literature ranges from 25 μg/kg·d to 8 mg/kg·d, and in this study we used the smallest dose ever attempted for in vivo experiments (25 μg/kg·d) (2, 19, 20). Therefore, even a low dose of FGF21 appeared to be sufficient to provide favorable metabolic effects on circulating levels of serum markers, although this dose was not sufficient to produce an expected weight loss.

Hale et al (6) recently observed that plasma levels of FGF21 are clearly elevated in diet-induced obesity (DIO) and *ob/ob* mice, but expression levels of β-Klotho and FGFRs are markedly down-regulated in the white adipose tissues of *ob/ob* and DIO mice. In this study, we observed that all FGF21-related components such as β-Klotho, FGFR1c, and FGFR2c were increased in the diabetic kidney compared with normal *db/m* mice, and FGF21 treatment significantly decreased β-Klotho, FGFR1c, and FGFR2c components. These results are in contrast with a previous study that found down-regulation of β-Klotho and FGFR receptors in liver and fat in DIO mice and *ob/ob* mice (6, 17). However, they did not observe the changes in kidney and used different animal models.

The above findings such as elevated FGF21 components in the diabetic kidney raised the question of how FGF21 could improve renal function. There is increasing evidence indicating that obesity is an FGF21-resistant state (16, 17), and exogenous FGF21 administration can overcome this FGF21 resistance. In this study, we used a dose of 25 μg/kg, and we further confirmed that FGF21 treatment activated ERK phosphorylation in the kidney. Taken together, these results suggest that the diabetic kidney is also an FGF21-resistant state and FGF21 treatment restores FGF21 sensitivity.

In this study, we observed that the renal FGF21 level in 20-week-old *db/m* mice is lower than that at 8-week-old *db/m* mice. The reason for the decreased expression of FGF21 in aged mice is not clear. However, we observed that cholesterol, triglycerides, and LPO content in renal cortical tissues was significantly higher in 8-week-old *db/m* mice compared with those in 20-week-old *db/m* mice (Supplemental Figure 7). There results agree with recent

reports that suggest the role of lipotoxicity and oxidative stress in up-regulation of FGF21 synthesis (22–24).

ERK1/2 is one of the MAPKs, and the ERK pathway is mainly activated by mitogenic stimuli including growth factors. Although there is a great deal of evidence implicating that activation of ERK1/2 may contribute to the development of human and experimental diabetic nephropathy (25, 26), it should be noted that ERK1/2 activation may not always result in tissue injury in the kidney (27). Furthermore, complex interaction of signaling networks activated in the diabetic kidney such as the different classes of MAPKs, phosphatidylinositide 3-kinase (PI3K)/AKT, and ERK1/2 pathways. Thus, it is likely that the activation of ERK1/2 may induce different protein synthesis and have a different physiological role in disease-specific manner.

Recent studies reported that serum FGF21 concentrations are elevated in patients with renal dysfunction, and serum FGF21 concentration correlates with renal function irrespective of the diabetic status (28, 29). The exact mechanism and physiological significance of increased serum FGF21 levels in patients with renal dysfunction are not clear, but there may be several possibilities. First, it may be possible that serum FGF21 concentrations are elevated due to limited clearance of FGF21 in the urine in patients with decreased renal function. Second, elevated FGF21 played a causative role in renal injury, but currently there is little evidence to support this hypothesis. Lastly, insulin resistance observed in renal failure leads to compensatory increase in FGF21 levels. However, the relationship between serum FGF-21 concentration and insulin resistance has not been explored in patients with renal disease. Future studies will be needed to determine the physiological significance of increased serum FGF21 levels in patients with renal dysfunction.

In this study, we observed that FGF21 treatment markedly decreased urinary albumin excretion as well as structural changes and oxidative stress in the kidney. Because FGF21 improved systemic insulin resistance and dyslipidemia, the renal protective effects of FGF21 are at least partly responsible for the improvement of systemic metabolic alterations. To further elucidate the direct effects of exogenous FGF21 on renal function, we performed additional in vitro experiments. We observed that FGF21 synthesis occurred exclusively in mesangial cells, and silencing of FGF21 in mouse MCs further aggravated synthesis of both high-glucose-induced fibrotic molecules synthesis. Taken together, these results suggest that exogenous FGF21 administration can provide direct renal protective effects in type 2 diabetic nephropathy.

Loeffler et al (30) recently reported that TGFβ1 stimulated MC proliferation and induced FGF21 expression via activation of MAPK and PI3K/AKT pathways in the absence of type VIII collagen. In addition, FGF21 mediates the shift from TGFβ1-induced Smad activation to the ERK1/2 and PI3K/AKT pathway, resulting in mesangial proliferation. It is generally considered that the sustained activation of repair mechanisms induces cell cycle arrest and increased extracellular matrix deposition, leading to irreversible renal fibrosis in the state of chronic kidney injury. This is further supported by the observation that diabetic p27Kip1 knockout mice have a reduced glomerular matrix expansion and less albuminuria despite an increase in the mesangial cell number compared with diabetic wild-type animals (31). Collectively these findings suggest the possibility that increased FGF21 expression may provide renal protective effect against progressive renal fibrosis.

In conclusion, we found that FGF21 treatment provided protective effects against diabetic kidney injuries as well as systemic insulin resistance and obesity-related type 2 diabetes, through both improvement of systemic metabolic alterations and antiinflammatory mechanisms. These findings suggest that FGF21 treatment could be a novel strategy targeting diabetic nephropathy in addition to various other diabetic complications.

Acknowledgments

Address all correspondence and requests for reprints to: Dae Ryong Cha, MD, Department of Internal Medicine, Korea University Ansan-Hospital, 516 Kojan-Dong, Ansan City, Kyungki-Do, 425–020, Korea. E-mail: cdragn@unitel.co.kr.

This work was supported by the Basic Science Research Program through the National Research Foundation of Korea funded by the Ministry of Education, Science, and Technology (Grant 2010–0009443).

Disclosure Summary: The authors have nothing to disclose.

References

1. **Itoh N, Ornitz DM.** Evolution of the Fgf and Fgfr gene families. *Trends Genet*. 2004;20:563–569.
2. **Kharitonenkov A, Shiyanova TL, Koester A, et al.** FGF-21 as a novel metabolic regulator. *J Clin Invest*. 2005;115:1627–1635.
3. **Badman MK, Pissios P, Kennedy AR, Koukos G, Flier JS, Maratos-Flier E.** Hepatic fibroblast growth factor 21 is regulated by PPARα and is a key mediator of hepatic lipid metabolism in ketotic states. *Cell Metab*. 2007;5:426–437.
4. **Cancilla B, Ford-Perriss MD, Bertram JF.** Expression and localization of fibroblast growth factors and fibroblast growth factor receptors in the developing rat kidney. *Kidney Int*. 1999;56:2025–2039.
5. **Cancilla B, Davies A, Cauchi JA, Risbridger GP, Bertram JF.** Fibroblast growth factor receptors and their ligands in the adult rat kidney. *Kidney Int*. 2001;60:147–155.

6. **Hale C, Chen MM, Stanislaus S, et al.** Lack of overt FGF21 resistance in two mouse models of obesity and insulin resistance. *Endocrinology*. 2012;153:69–80.
7. **Bligh EG, Dyer WJ.** A rapid method of total lipid extraction and purification. *Can J Biochem Physiol*. 1959;37:911–917.
8. **Kang YS, Lee MH, Song HK, et al.** CCR2 antagonism improves insulin resistance, lipid metabolism, and diabetic nephropathy in type 2 diabetic mice. *Kidney Int*. 2010;78:883–894.
9. **Han SY, Kim CH, Kim HS, et al.** Spironolactone prevents diabetic nephropathy through an anti-inflammatory mechanism in type 2 diabetic rats. *J Am Soc Nephrol*. 2006;17:1362–1372.
10. **Hajer GR, van Haeften TW, Visseren FL.** Adipose tissue dysfunction in obesity, diabetes, and vascular diseases. *Eur Heart J*. 2008;29:2959–2971.
11. **Roberts CK, Sindhu KK.** Oxidative stress and metabolic syndrome. *Life Sci*. 2009;84:705–712.
12. **Morrow JD, Roberts LJ.** The isoprostanes: unique bioactive products of lipid peroxidation. *Prog Lipid Res*. 1997;36:1–21.
13. **Betteridge DJ.** What is oxidative stress? *Metabolism*. 2000;49:3–8.
14. **Ouchi N, Walsh K.** Adiponectin as an anti-inflammatory factor. *Clin Chim Acta*. 2007;380:24–30.
15. **Wang Z, Jiang T, Li J, et al.** Regulation of renal lipid metabolism, lipid accumulation, and glomerulosclerosis in FVBdb/db mice with type 2 diabetes. *Diabetes*. 2005;54:2328–2335.
16. **Zhang X, Yeung DC, Karpisek M, et al.** Serum FGF21 levels are increased in obesity and are independently associated with the metabolic syndrome in humans. *Diabetes*. 2008;57:1246–1253.
17. **Fisher FM, Chui PC, Antonellis PJ, et al.** Obesity is a fibroblast growth factor 21 (FGF21)-resistant state. *Diabetes*. 2010;59:2781–2789.
18. **Sarafidis PA.** Obesity, insulin resistance and kidney disease risk: insights into the relationship. *Curr Opin Nephrol Hypertens*. 2008;17:450–456.
19. **Coskun T, Bina HA, Schneider MA, et al.** Fibroblast growth factor 21 corrects obesity in mice. *Endocrinology*. 2008;149:6018–6027.
20. **Xu J, Lloyd DJ, Hale C, et al.** Fibroblast growth factor 21 reverses hepatic steatosis, increases energy expenditure, and improves insulin sensitivity in diet-induced obese mice. *Diabetes*. 2009;58:250–259.
21. **Do HT, Tselykh TV, Makela J, et al.** Fibroblast growth factor-21 (FGF21) regulates low-density lipoprotein receptor (LDLR) levels in cells via the E3-ubiquitin ligase Mylip/Idol and the Canopy2 (Cnpy2)/Mylip-interacting saposin-like protein (Msap). *J Biol Chem*. 2012;287:12602–12611.
22. **Chartoumpekis DV, Ziros PG, Psyrogiannis AI, et al.** Nrf2 represses FGF21 during long-term high-fat diet-induced obesity in mice. *Diabetes*. 2011;60:2465–2473.
23. **Gaemers IC, Stallen JM, Kunne C, Wallner C, Werven JV, Nederveen A, Lamers WH.** Lipotoxicity and steatohepatitis in an overfed mouse model for non-alcoholic fatty liver disease. *Biochim Biophys Acta*. 2011;1812:447–458.
24. **Schaap FG, Kremer AE, Lamers WH, Jansen PLM, Gaemers IC.** Fibroblast growth factor 21 is induced by endoplasmic reticulum stress. *Biochimie*. 2013;95:692–699.
25. **Sakai N, Wada T, Furuichi K, et al.** Involvement of extracellular signal-regulated kinase and p38 in human diabetic nephropathy. *Am J Kidney Dis*. 2005;45:54–65.
26. **Lin CL, Wang FS, Kuo YR, et al.** Ras modulation of superoxide activates ERK-dependent fibronectin expression in diabetes-induced renal injuries. *Kidney Int*. 2006;69:1593–1600.
27. **Kunduzova OR, Bianchi P, Pizzinat N, et al.** Regulation of JNK/ERK activation, cell apoptosis, and tissue regeneration by monoamine oxidases after renal ischemia-reperfusion. *FASEB J*. 2002;16:1129–1131.
28. **Crasto C, Semba RD, Sun K, Ferrucci L.** Serum fibroblast growth factor 21 is associated with renal function and chronic kidney disease in community-dwelling adults. *J Am Geriatr Soc*. 2012;60:792–793.
29. **Han SH, Choi SH, Cho BJ, et al.** Serum fibroblast growth factor-21 concentration is associated with residual renal function and insulin resistance in end-stage renal disease patients receiving long-term peritoneal dialysis. *Metabolism*. 2010;59:1656–1662.
30. **Loeffler I, Hopfer U, Koczan D, Wolf G.** Type VIII collagen modulates TGF-β1-induced proliferation of mesangial cells. *J Am Soc Nephrol*. 2011;22:649–663.
31. **Wolf G, Schanze A, Stahl RAK, Shankland SJ, Amann K.** p27Kip1 knockout mice are protected from diabetic nephropathy: evidence for p27Kip1 haplotype insufficiency. *Kidney Int*. 2005;68:1583–1589.